Preparation of Highly Ordered Vanadium-Substituted MCM-41: Stability and Acidic Properties†

Sangyun Lim and Gary L. Haller*

Department of Chemical Engineering, Yale University, 9 Hillhouse Avenue, New Haven, Connecticut 06520-8286

Received: April 16, 2002; In Final Form: June 10, 2002

Vanadium-substituted mesoporous molecular sieves (MCM-41) were prepared and the effects of water concentration, anti-foaming agent addition, pH adjustment, and Si/surfactant mole ratio were investigated. The hydrothermal and mechanical stability were tested for the pH-adjusted sample (Si/surfactant = 3.67 and 7.34). Catalysts were characterized by XRD, N_2 physisorption, ICP, and ^{51}V NMR. The acidic properties of synthesized V−MCM-41 were also examined by in-situ FTIR and TPD after pyridine adsorption. The increase of water concentration in the synthesis solution did not affect the physical properties of the resulting samples. The anti-foaming agent was very effective in improving the reproducibility of sample structure. The degree of vanadium substitution in the silica framework was increased with increasing water concentration and surfactant chain length. All of the incorporated vanadium was tetrahedrally coordinated in the silica framework. When the pH of the synthesis solution for V−MCM-41 was adjusted to 11 (Si/surf. = 7.34), the hydrothermal and mechanical stability were enhanced. The vanadium-substituted MCM-41 formed Lewis and Brönsted acid sites. Brönsted acid sites increased with increasing vanadium content, but the density of Lewis acid sites was constant for all samples. It is hypothesized that there is formed a constant and saturated density of isolated tetrahedral coordinated vanadium, and these make weak Lewis acid sites. Brönsted acid sites can be formed by a combination of incorporated vanadium with a hydroxyl group of a free silanol and/or a hydroxyl group produced by dissociation of water when the sample was pretreated at high temperature.

Introduction

There has been a great deal of research and numerous publications on the synthesis, characterization, and properties of the material labeled M41S since Mobil researchers disclosed this surprising material.[1,2] The hexagonal structured member of this family of materials, MCM-41, has been an especially popular mesoporous molecular sieve because of the possibility of its catalytic application. Thus, many researchers have tried to introduce a second cation, such as a transition metal, into the silica-based MCM-41 framework[3−10] and have used them as effective catalysts for various kinds of reactions.[11−15] MCM-41 has a very flexible framework structure, compared to crystalline zeolites, allowing various kinds of metals to be incorporated into the silica framework without collapse of its basic structure when the preparation conditions are carefully controlled. The decisive factors for preparing metal-containing MCM-41 with a highly ordered hexagonal pore structure are synthesis solution composition, pH, temperature, and other additives such as water, organic compounds, etc. Excess foam, which results from the surfactant templating agent, has been a particular problem requiring solution in order to obtain sample reproducibility. Mobil scientists suggested an anti-foaming agent as a method to solve this problem.[16] The temperature of synthesis is one of the most important variables which must be controlled to obtain a highly ordered hexagonal pore structure in MCM-41 because of its effect on the degree of condensation of silanol groups.[17,18] The attainment of a highly ordered MCM-41 structure is also dependent on the pH of the synthesis solution, in addition to the temperature.[19] It is generally thought that the increase in concentration of water in the synthesis solution is not desirable to achieve high regularity of MCM-41, but this is unclear to date.

The acidic properties of the metal-substituted MCM-41 are very important for catalytic application to certain reactions. In commercial catalyst applications, the mechanical strength is crucial as well as is the hydrothermal stability. Several results concerning the mechanical strength of mesoporous molecular sieves (MCM-41 or MCM-48) have been reported in the past few years,[20−22] but metal-substituted MCM-41 has not been investigated so far. According to previous research, MCM-48 is more stable than MCM-41 under mechanical pressure. In many cases, it is known that the pore size of metal-substituted MCM-41 is decreased and the pore size distribution becomes broad relative to the pure siliceous MCM-41. The perturbation of pore size is hypothesized to be dependent on the metal substitution state resulting from the sample preparation method, i.e., coordination number of metal with OH groups on the silica surface.

In this study, we have focused on the preparation of highly ordered, metal-substituted MCM-41, in particular, V-containing MCM-41. The possibility of preparing V-incorporated MCM-41 was reported by Sayari in 1994,[23] and thereafter several reports about V−MCM-41 have been published.[24−29] However, there are few results claiming successful preparation of V−MCM-41 with high reproducibility and mechanical stability nor has a systematic investigation of acidic properties relevant to catalytic applications been presented. Therefore, with the goal of preparing highly ordered V−MCM-41 and determining effects on mechanical and hydrothermal stability, we have investigated the

† Part of the special issue "John C. Tully Festschrift".
* Author to whom correspondence should be addressed.

10.1021/jp0209796 CCC: $22.00
Published on Web 07/16/2002

effects of synthesis solution water concentration, pH adjustment, and Si/surfactant mole ratio. Changes of V incorporation amount accompanying different surfactant chain length, anti-foaming agent addition effects for increasing reproducibility, and the acidic properties of V−MCM-41 which may be relevant to its properties as an oxidation catalyst are also reported.

Experimental Section

Materials. Silica sources were HiSil-233 (or HiSil-915) from Pittsburgh Plate Glass (PPG) and tetramethylammonium silicate (10 wt % silica, SACHEM Inc.). The V source was $VOSO_4 \cdot 3H_2O$ (Aldrich Chemical Co.). The quaternary ammonium surfactants $C_nH_{2n+1}(CH_3)_3NBr$ were purchased from Sigma Co. with $n = 12$, 14, 16 and from American Tokyo Kasei with $n = 10$. The surfactant solutions were prepared by ion-exchanging 29 wt % $C_nH_{2n+1}(CH_3)_3NBr$ aqueous solution with equal molar exchange capacity of Amberjet-400 (OH) ion-exchange resin (Sigma Co.) by overnight batch mixing. The anti-foaming agent was Antifoam A from Sigma Co., a silane polymer alkyl terminated by methoxy groups. Acetic acid (Fisher Scientific) was used for pH adjustment of the synthesis solution.

Synthesis. HiSil-233 (or HiSil-915), tetramethylammonium silicate, and the V aqueous solution were mixed for 30 min. To investigate the effect of water concentration, the water-to-silicon ratio was varied from H_2O/Si mole ratio = 27 to 74.7, based on the H_2O/Si mole ratio = 27 as the reference, i.e., ratios greater than 27 are said to have "excess water." The surfactant solution was added to the prepared silica and V mixture and a small amount of anti-foaming agent (0.2 wt % of surfactant) was added to remove excess foam produced by the surfactant. To investigate the effect of pH adjustment, acetic acid was added until pH = 11 was reached. After additional mixing for about 10 min, this synthesis solution was poured into a polypropylene bottle and placed in the autoclave at 100 °C for 6 days. After cooling to room temperature, the resulting solid was recovered by filtration, washed with deionized water, and dried under ambient conditions. The predried solid was calcined by heating from room temperature to 540 °C over 20 h under He, 1 h at 540 °C with He, and 5 h at 540 °C with air to remove the residual surfactant. The molar ratio of each component in the synthesis solution was controlled at SiO_2:surfactant:V:H_2O = 1:0.27:0.017:X (X = 27−74.7). The preparation process may cause some loss of V and silica in the byproducts, so the V content of each sample was measured by ICP (Galbraith Lab., Inc.). A pure siliceous MCM-41 was also prepared with the same procedure as used for V−MCM-41 except without addition of vanadium to the synthesis solution.

Characterization. *N_2 Physisorption*. Adsorption−desorption isotherms of N_2 at 77 K were measured with a static volumetric instrument Autosorb-1C (Quantachrome). The samples were outgassed at 200 °C to a residual pressure lower than 1×10^{-4} Torr. A Baratron (0.001−10 Torr) pressure transducer was used for low-pressure measurements. The pore size and its distributions were calculated by the BJH method using the desorption isotherm. It is well-known that the BJH method results in an under-estimation of the diameter of mesopores, and Ravikovitch et al.[25] have reported that nonlocal density functional theory (NLDFT) is a reliable method for the measurement of mesopore size. In this study, we did not focus on the pore size measurement of synthesized samples, so the BJH method was used for the relative pore size measurement of each sample. For the investigation of the sample stability (mechanical and hydrothermal), samples were pressed with varying pressure from 849−4640 atm (which corresponds to 878−4800 kg/cm^2), and/or boiled for 24 h in water. These samples were analyzed by N_2 physisorption to compare the adsorption isotherm patterns with fresh samples.

XRD. To determine if the prepared V−MCM-41 has the characteristic hexagonal pore structure after calcination, X-ray diffraction measurement was carried out by a SCINTAG X-ray diffractometer (Cu Kα, λ = 0.154 nm, 40 kV, 45 mA). From the results of XRD and N_2 physisorption, the pore wall spacing was calculated by using the relationship between the lattice parameter and d spacing. ($a_o = 2d_{100}/\sqrt{3}$)

^{51}V NMR. The solid ^{51}V NMR spectra were recorded at room temperature using an Am-500 Bruker spectrometer (11.7 T) at 131.44 MHz equipped with multinuclear MAS probe from Doty Scientific Inc. A 5 mm standard zirconia rotor was used. Chemical shifts were referenced against liquid $VOCl_3$ by using ammonium metavanadate (NH_4VO_3, $\delta = -576$ ppm at 11.7 T) as a secondary reference. The 90 degree pulse length was measured with the solution and solid of the standard sample. According to ref 30, to avoid distortion of the signal caused by selective excitation, a shorter pulse length was applied in data accumulation by using a single pulse sequence. The spectra were obtained with a pulse length of 1.1 μs equivalent to about a 40 degree pulse. The relaxation delay was 0.5−1 s; the spectral width was chosen as 166.7 kHz and 1000 data points were used.

Pyridine TPD and in-Situ FTIR. The acid site density and acid strength of synthesized V−MCM-41 were measured by temperature-programmed desorption (TPD) of pyridine and in-situ FTIR, respectively. A home constructed flow reactor system connected to a gas chromatograph (HP6890) was used for TPD experiment. Two-hundred milligrams of catalyst was charged in a quartz reactor and pretreated with ultrahigh purity He at 500 °C for 1 h. In this study, pyridine was used as an adsorbate to correlate directly with the results of in-situ FTIR after pyridine adsorption on the prepared catalyst. To prevent the condensation of pyridine on the catalyst surface, the adsorption temperature of pyridine was chosen as 150 °C. After 30 min of pyridine exposure, the physisorbed pyridine was flushed out by a high flow rate of He for 1 h. The temperature ramp rate was 5 °C/min and the carrier gas (He) flow rate was 40 mL/min. The acid strength and the kinds of acid sites were characterized by in-situ FTIR after pyridine adsorption on the catalyst. A MIDAC M series spectrometer was used for this experiment. Fifty milligrams of sample was pressed at 800 Kg/cm^2 into a thin wafer and installed in a stainless steel cell. The adsorption and desorption conditions for the in-situ FTIR was exactly the same as for the TPD experiment. The spectra were recorded in nitrogen at room temperature in the absorbance mode in the range of 1400−1650 cm^{-1} for acid sites and 3000−4000 cm^{-1} for hydroxyl group with a spectral resolution of 0.5 cm^{-1}.

Results and Discussion

XRD. After calcination of each sample, the XRD spectrum was obtained to confirm the hexagonal structure of MCM-41 and the results are shown in Figure 1. When the anti-foaming agent was not added to the synthesis solution, the XRD patterns are different when the samples with different H_2O/Si mole ratio are compared ((a) of Figure 1). When there is no additional water (relative to the reference H_2O/Si mole ratio of 27) in the synthesis solution, the XRD pattern shows only one broad peak at around $2\theta = 2.5$ which is assigned to the (100) reflection. By adding excess water to obtain a H_2O/Si mole ratio = 74.7, the XRD pattern exhibits a very highly ordered hexagonal pore structure. This suggests that the addition of excess water is very helpful to obtain a more homogeneous synthesis solution.

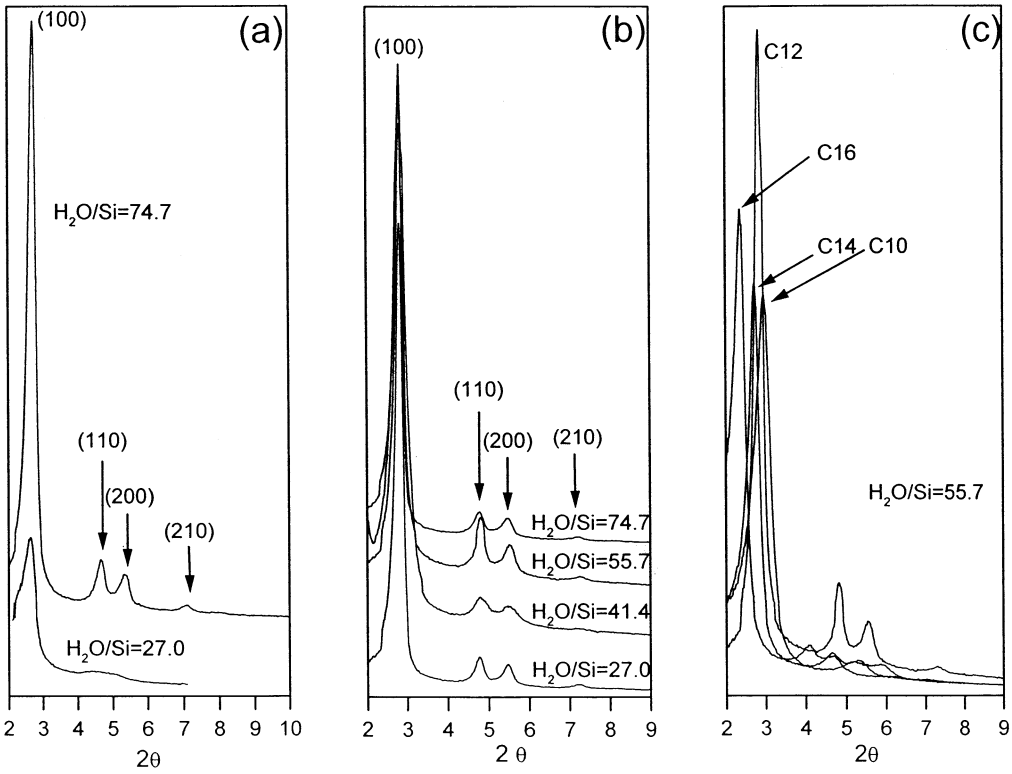

Figure 1. XRD patterns of calcined V−MCM-41 samples: (a) without anti-foaming agent (C12 V−MCM-41); (b) with anti-foaming agent (C12 V−MCM-41); (c) with anti-foaming agent, H_2O/Si mole ratio = 55.7 (C10−16 V−MCM-41).

However, the reproducibility of this preparation method was not good. The water-related mixing effect will be discussed in a later section.

When the anti-foaming agent was added to the synthesis solution, the XRD patterns of all samples show a highly ordered hexagonal structure. As shown in Figure 1b, C12 V−MCM-41 samples prepared with anti-foaming agent and different water addition amounts have exactly the same XRD patterns and also the same *d* spacing values. This result demonstrates that when the anti-foaming agent is used, the reproducibility of samples, by this method of preparation, is increased compared to the samples prepared without the anti-foaming agent. This result also shows that the addition of water to the synthesis solution does not affect the physical properties of V−MCM-41 samples in the presence of the anti-foaming agent. When the same method was applied to C10, C14, and C16 surfactants, all prepared samples also have highly ordered hexagonal structures as shown in Figure 1c. Even the C10 sample shows (110) and (200) reflections in addition to the (100) reflection, although it produces a highly ordered MCM-41 structure with more difficulty compared to the long chain length surfactants. As may be expected, *d* spacing of each sample is increased with increased surfactant chain length. The calculated lattice parameters (a_o) from this XRD experiment are discussed later.

Usually, pH adjustment is considered as a crucial factor in the synthesis of MCM-41 with a highly ordered hexagonal pore structure. In this study, we could obtain highly ordered V−MCM-41 samples regardless of the surfactant chain length (C10−C16) without pH adjustment (pH ≅ 13), i.e., without addition of acid to the synthesis solution.

The pH adjustment effect was investigated for C14 and C16 V−MCM-41 samples, and the results are shown in Figure 2a,b. The diffraction pattern of pH-adjusted samples is more distinct than is the case for nonadjusted samples, and the peaks are shifted to lower angle after pH adjustment. One consequence of pH adjusted to 11 is known, i.e., that silica is dissolved in the synthesis solution at pH higher than 11, and most silica is precipitated around pH = 11.[31] When the synthesis solution without pH adjustment was mixed over 10 min, it became very viscous, but did not if the pH was adjusted to 11. This suggests that a lower silica concentration in solution results in a slower re-polymerization and precipitation of the MCM-41 structure and that this is beneficial. That is, pH-adjusted samples seem to show higher structured hexagonal pore arrangement and reproducibility than nonadjusted samples.

The effect of Si/surfactant mole ratio was investigated for C14 V−MCM-41 samples. Most samples in this study were prepared on the basis of a reference Si/surfactant = 3.67, and this was increased to 29.36 to compare the physical properties with the reference sample. We find that the Si/surfactant mole ratio is one of the crucial factors in the synthesis of highly structured V−MCM-41. When the Si/surfactant mole ratio was 14.68, the structure of MCM-41 appears to begin to collapse, and it was completely absent at Si/surfactant = 29.36. When we decreased the surfactant amount to half that used in the reference sample, there was no significant difference in physical properties (XRD and N_2 physisorption), but the XRD peak intensity was decreased a little as shown in Figure 2c. This experiment was simply carried out as a possible method to increase physical strength. That is, decreasing the amount of surfactant in a range where the MCM-41 structure is maintained with a fixed silica amount may result in increased pore wall thickness or a change of silanol group condensation because of the relatively high concentration of silica compared to the reference sample (Si/surfactant = 3.67). This will be discussed also in a later section.

It is well-known that incorporation of a transition metal into siliceous MCM-41 results in a decreased (most often observed) or increased pore size. In the crystalline zeolites, metal incorporation slightly increases the pore size because of its

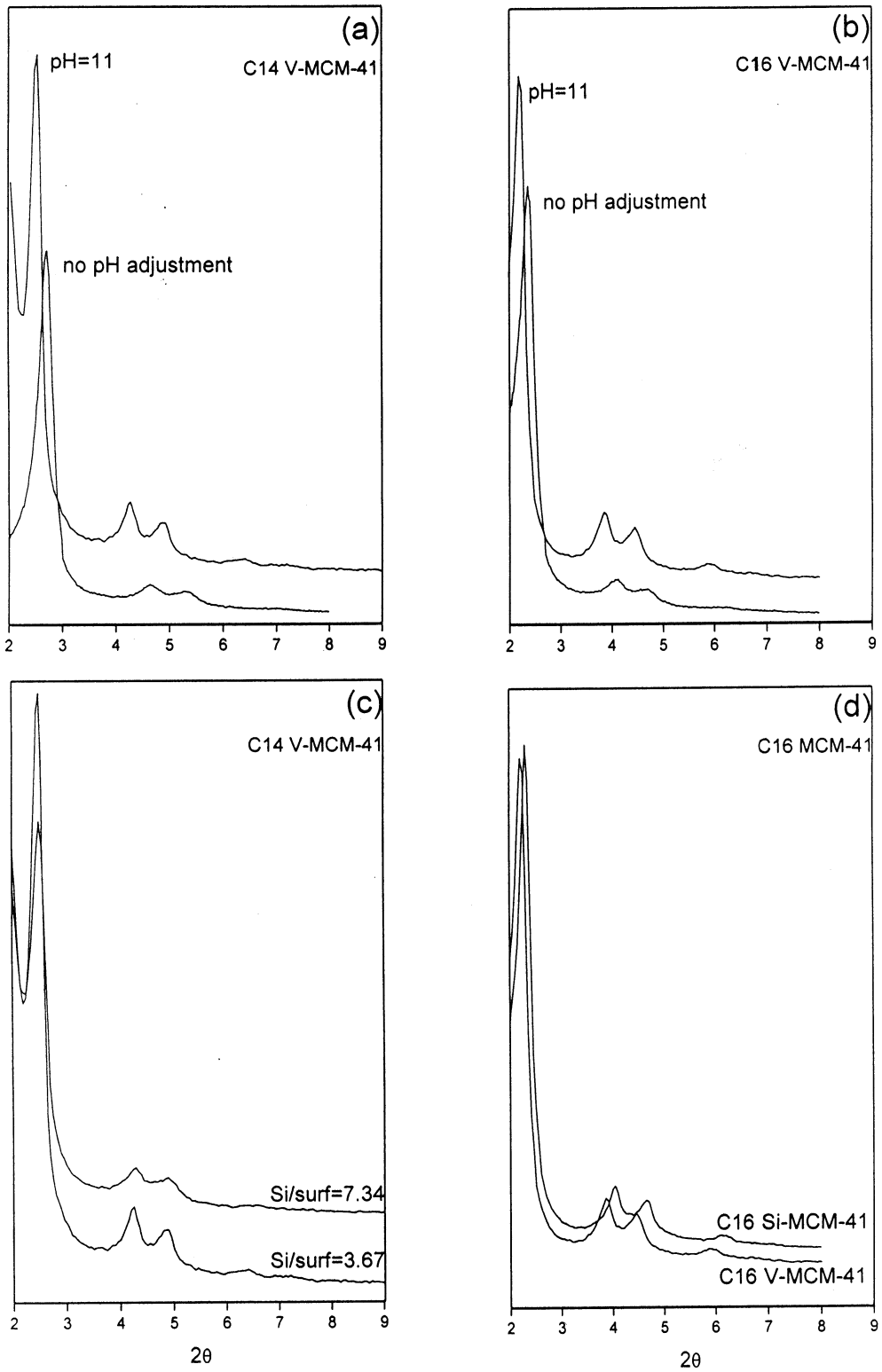

Figure 2. XRD patterns of calcined C14 and C16 V−MCM-41 samples: (a) pH adjustment effect of C14 V−MCM-41with anti-foaming agent (H_2O/Si mole ratio = 74.7); (b) pH adjustment effect of C16 V−MCM-41with anti-foaming agent (H_2O/Si mole ratio = 74.7); (c) Si/surfactant mole ratio effect of C14 V−MCM-41with anti-foaming agent (H_2O/Si mole ratio = 74.7, pH = 11); (d) vanadium addition effect of C16 MCM-41with anti-foaming agent (H_2O/Si mole ratio = 74.7, pH = 11).

longer bonding length with oxygen than Si−O. However, there is no regular rule in MCM-41 as it has an amorphous structure where both bond length and angle may change. Usually, it has been observed that the pore size of MCM-41 is decreased after metal incorporation, but there is no clear explanation for this observation. MCM-41 has thin pore walls relative to zeolites so that the incorporated metal cannot be substituted into the silica framework completely. That is, a part of the metal will be exposed on the pore wall surface so that it might have properties similar to impregnated metal complexes on the MCM-41 walls. The incorporated metal may interact with surface hydroxyl groups and may contract the pore wall when combined with two or three hydroxyl groups, so that the pore size will be decreased.[32] If these metals are incorporated deep within the

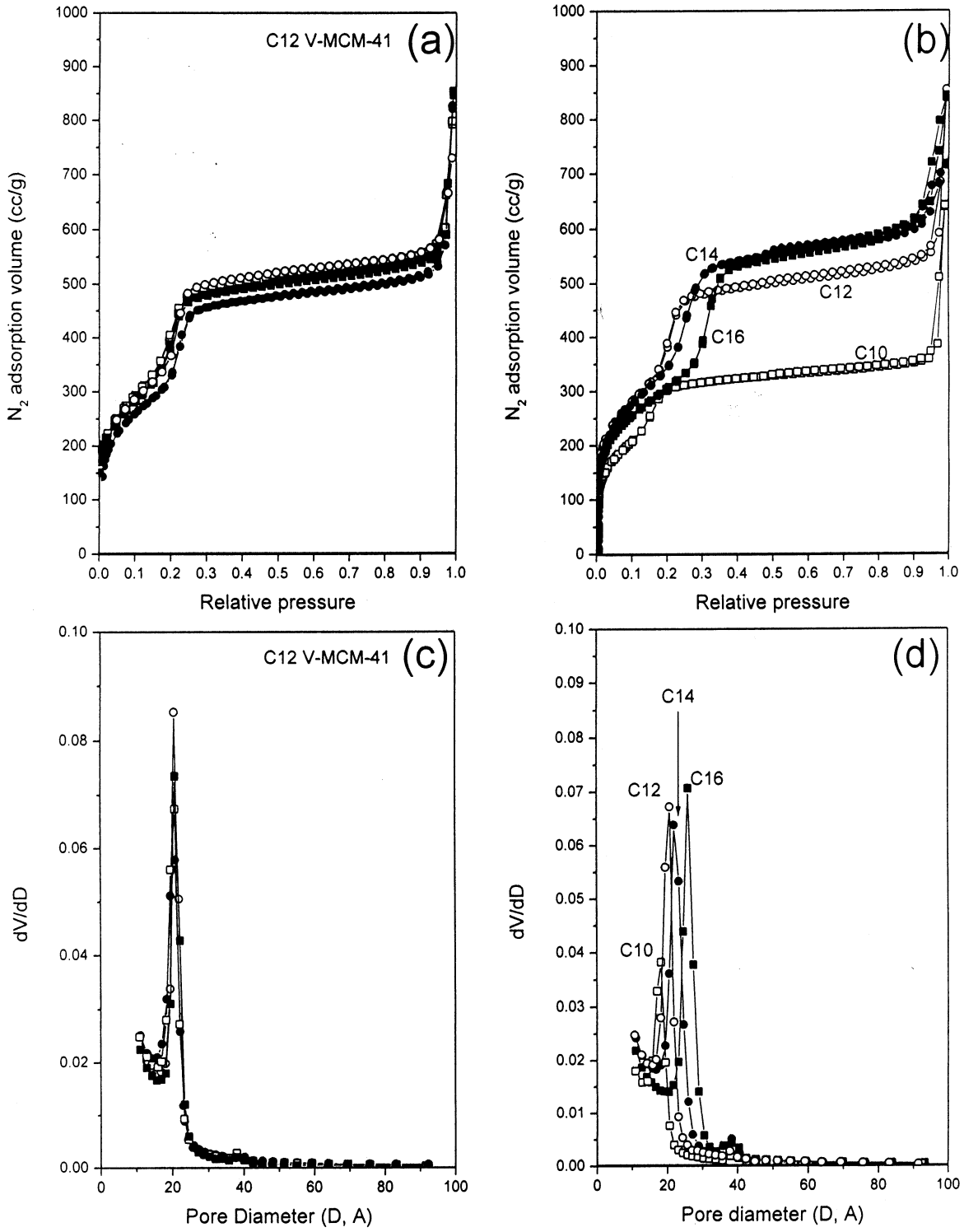

Figure 3. N_2 physisorption patterns and pore size distributions of V−MCM-41 samples: (a) adsorption isotherms of C12 V−MCM-41, with anti-foaming agent (□ H_2O/Si mole ratio = 27, ○ H_2O/Si mole ratio = 41.4, ● H_2O/Si mole ratio = 55.7, ■ H_2O/Si mole ratio = 74.7); (b) adsorption isotherms of C10−16 V−MCM-41 samples (□ C10, ○ C12, ● C14, ■ C16), with anti-foaming agent (H_2O/Si mole ratio = 55.7); (c) pore size distributions of C12 V−MCM-41, with anti-foaming agent (□ H_2O/Si mole ratio = 27, O H_2O/Si mole ratio = 41.4, ● H_2O/Si mole ratio = 55.7, ■ H_2O/Si mole ratio = 74.7); (d) pore size distributions of C10−C16 V−MCM-41 samples (□ C10, ○ C12, ● C14, ■ C16), with anti-foaming agent (H_2O/Si mole ratio = 55.7).

silica framework, this pore shrinkage might not occur as with condensed surface hydroxyl groups, and the pore size might be increased instead by the increased metal−oxygen bond length, as for zeolites. In this study, we obtained an increased pore size after vanadium incorporation as shown in Figure 2d. This is an unusual result, and strongly suggests that vanadium is incorporated into silica framework according to the above hypothesis. This can be confirmed indirectly by the ease of metal reduction, and such a result has been reported.[33]

N_2 Physisorption. As another method to confirm the highly ordered MCM-41 structure, the nitrogen physisorption technique may be used because the structure of MCM-41 contains a regular pore arrangement so that it has the typical characteristics of capillary condensation. Therefore if the synthesized sample has

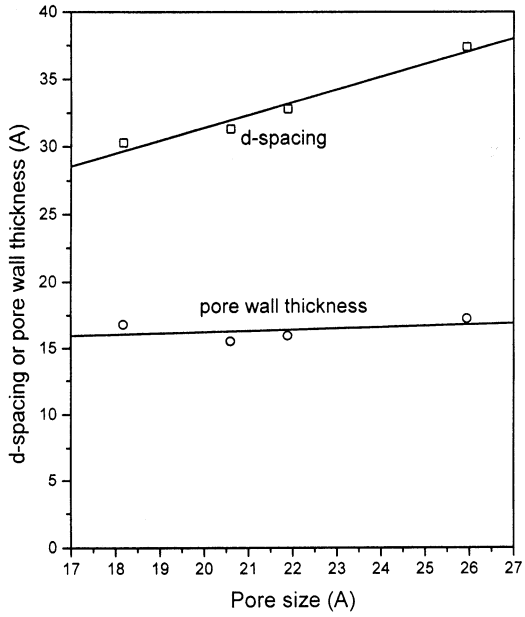

Figure 4. Plot of pore size vs *d* spacing and pore wall thickness.

a regular pore structure it should show a step increase in the adsorption isotherm due to the capillary condensation at a certain N_2 partial pressure. The nitrogen adsorption isotherms of C12 V−MCM-41 samples prepared by adding anti-foaming agent and excess water are shown in Figure 3a. All isotherms show a step increase at around a relative pressure = 0.2. This demonstrates that all samples prepared by our recipe have highly ordered regular pore structures. There is also a step increase at around a relative pressure = 0.9−1. This is due to the macropore filling, which is produced by interparticle spacing. As seen in the XRD results, all adsorption isotherms of C12 samples show almost identical patterns. This shows that the samples prepared with the anti-foaming agent can be highly reproducible regardless of the water/Si mole ratio in the synthesis mixture. When we compared the pore size distributions of C12 V−MCM-41 samples as shown in Figure 3c, the main pore size of each sample is exactly the same, 21 Å. From this result, it can be predicted that the pore wall thickness of these samples is the same. It may be concluded that the addition of anti-foaming agent is helpful to increase the reproducibility of the prepared samples and that excess water does not affect the physical properties of V−MCM-41 samples when the anti-foaming agent is used. The nitrogen physisorption results of each sample prepared by different surfactant chain length and their pore size distributions are shown in Figure 3b,d. The relative pressure, which corresponds to the capillary condensation of each sample, is shifted to a higher pressure as the surfactant chain length is systematically increased. The pore size increases with increasing surfactant chain length from 18.2 Å to 25.9 Å. When this result is compared to the XRD patterns, it can be concluded that all prepared samples show a similar pore wall thickness regardless of surfactant chain length. The *d* spacing of samples prepared by different surfactant chain length is increased linearly with increasing pore diameter (see Figure 4). Therefore, the pore wall thickness, which is calculated from *d* spacing and pore diameter, shows a constant value. From these results, it is concluded that the preparation method of V−MCM-41 with anti-foaming agent is very highly reproducible and produces constant physical properties for all samples.

Nitrogen physisorption experiments were carried out for pH-adjusted samples (C14 and C16 V−MCM-41), and the results are shown in Figure 5. Both samples show smaller nitrogen adsorption amount and a sharp capillary condensation without any hysteresis loop in the high relative pressure range, compared to the pH-nonadjusted samples. This indicates that there is no interparticle space in the pH-adjusted samples, and this may be attributed to the homogeneous mixing of the lower pH synthesis. The pore diameter was increased when pH was adjusted, and this might be due to the difference of vanadium substitution state. Vanadium can be incorporated into siliceous MCM-41 in two ways. It may be distributed along the pore walls and combined with hydroxyl groups to make tetrahedral coordination (contracting the pore walls) or it may be incorporated into silica framework with tetrahedral coordination. The distribution might depend on the mixing effect of the synthesis solution. Therefore, when we consider the mixing effectiveness between two samples, vanadium incorporated into the pH-adjusted sample may be preferentially distributed in the silica framework rather than on the pore wall surface, and thus exhibits a larger pore size than pH-nonadjusted sample.

Effects of Si/surfactant mole ratio and vanadium incorporation were investigated by nitrogen physisorption as shown in Figure 6. To test the possibility of controlling the pore wall thickness, simply by changing Si/surfactant mole ratio, we decreased the surfactant amount step by step until it equaled one-quarter of the reference sample (Si/surf. = 3.67). When the Si/surfactant mole ratio is 14.68 (see Figure 6a), the nitrogen adsorption amount is severely decreased, and the adsorption isotherm shows no capillary condensation at Si/surf. = 29.36. This result indicates that there is a limitation in controlling the pore wall thickness by reducing the surfactant amount. When the Si/surfactant mole ratio is 7.34, the adsorption isotherm is almost the same as the reference sample. All samples show similar pore sizes regardless of Si/surfactant mole ratio (see Table 1), which implies that Si/surfactant mole ratio does not affect the pore size. From this result, we may expect some differences in properties between the reference and Si/surf. = 7.34 samples. Figure 6b,d shows the nitrogen adsorption isotherms and pore size distributions of siliceous MCM-41 and vanadium-incorporated MCM-41 samples. When vanadium is incorporated into siliceous MCM-41, the nitrogen adsorption volume is decreased a little, and the pore size is increased. These results may have an interpretation related to the vanadium bonding state, as discussed in the XRD section.

To test the hydrothermal stability of V−MCM-41 samples, two samples (C14 V−MCM-41, Si/surf. = 3.67 and 7.34) were boiled for 24 h in water (see Figure 7). The nitrogen adsorption isotherms of these samples are shown in Figure 7. In this harsh environment, most MCM-41 structures completely collapse. However, when the Si/surfactant mole ratio is 7.34, both fresh and boiled samples exhibit capillary condensation, and the adsorption isotherm difference between fresh and boiled samples is quite small, i.e., except for a slight broadening of pore size distribution, the samples are about the same. This may be related to the degree of silanol group condensation. That is, when the Si/surfactant mole ratio is 7.34, the relative silica amount is higher than the Si/surf. = 3.67 sample. Thus, the chance of the silanol group condensation may be greater than that for the reference sample, and it may be more stable in the hydrothermal treatment. This catalyst has already been demonstrated to be quite stable at the practical reaction temperature (350 °C) under gas-phase methanol oxidation that produces water as a main product.[34] From this result, we may expect increased mechanical stability for this sample which is a requirement for useful catalytic applications.

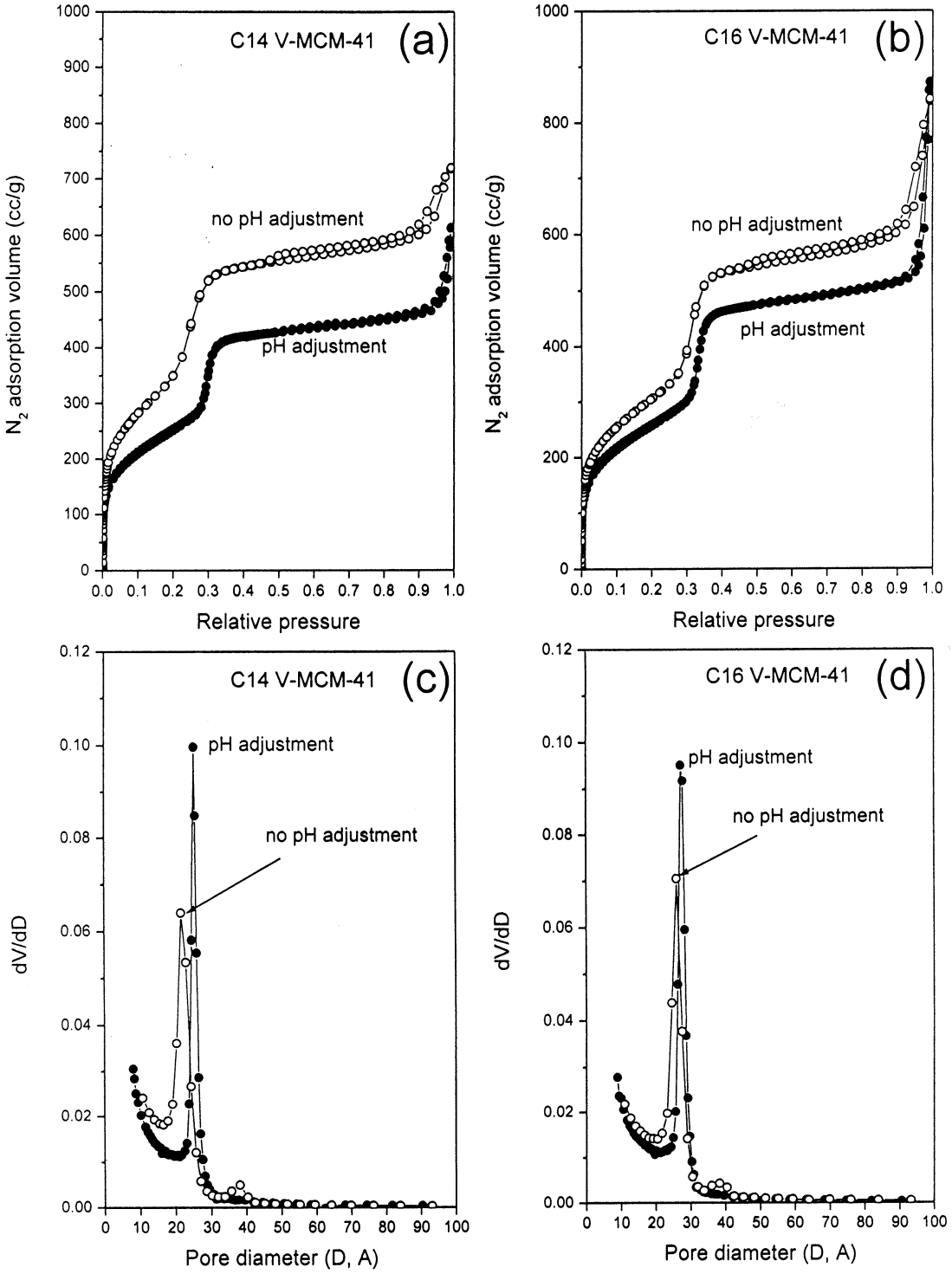

Figure 5. Nitrogen adsorption isotherms and pore size distributions of C14 and C16 V−MCM-41 samples (pH adjustment effect).

To investigate the mechanical stability, we pressed samples (C14 V−MCM-41, Si/surf. = 3.67 and 7.34) with varying pressure from 878 to 4800 Kg/cm^2 and carried out nitrogen physisorption as shown in Figure 8. When the sample of Si/surf. = 7.34 was pressed with 878 Kg/cm^2, the nitrogen adsorption amount is decreased, but the capillary condensation is observed at the same relative pressure. When we consider that there is no great difference in surface area of these samples, this decreased adsorption amount is due to loss of interparticle space resulting from compression. There is no change in the adsorption isotherm up to 3400 Kg/cm^2, and then it begins to decrease a little from 4000 Kg/cm^2 and 4800 Kg/cm^2. There is still a sharp capillary condensation even at 4800 Kg/cm^2, and when we consider that all samples show similar surface areas, regardless of pressure (see Table 1), we can suggest that V−MCM-41 prepared in this study has good hydrothermal and mechanical stabilities. Our samples appear to be more stable in mechanical strength than MCM-48 reported recently.[21,22] Relative to this sample (Si/surf. = 7.34), the reference sample (Si/surf. = 3.67) shows less mechanical strength (Figure 8b). This may be due to the difference in the degree of the silanol group condensation, as mentioned earlier. When we tested the pH-nonadjusted samples, they showed complete collapse with the lowest pressure (878 Kg/cm^2). This may be the result of

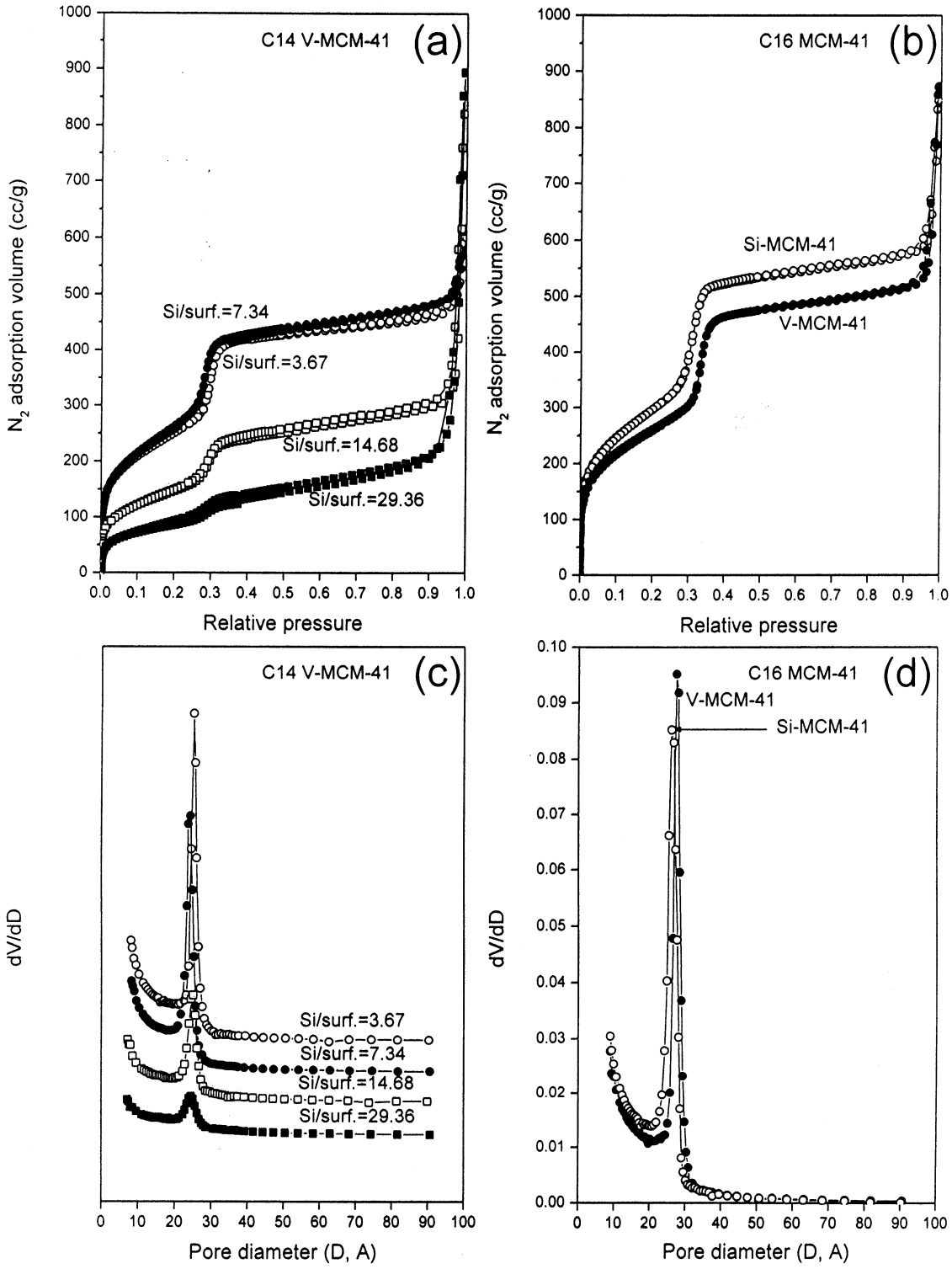

Figure 6. Nitrogen adsorption isotherms and pore size distributions of V−MCM-41 samples.: (a), (c) C14 V−MCM-41 (○ Si/surf. = 3.67, ● Si/surf. = 7.34, □ Si/surf. = 14.68, ■ Si/surf. = 29.36), Si/surf. Mole ratio effect; (b), (d) C16 V−MCM-41, vanadium addition effect.

dissolved silica in the synthesis solution because the high pH value (around 13) results in less silanol group condensation than occurred with pH-adjusted samples, as discussed in the XRD section. The silanol group condensation will be confirmed by ^{29}Si MAS NMR.

Water Addition Effect (Results of ICP Analysis). In the previous results, we could not see any changes in the physical properties of synthesized samples with increased H_2O/Si ratio used in the synthesis solution with added anti-foaming agent. We must question if there is, in fact, any effect of excess water on the preparation of V−MCM-41. To confirm the amount of V incorporated into siliceous MCM-41, a chemical analysis method (ICP) for V detection was carried out. When C12 V−MCM-41 samples prepared with different water addition amounts are compared, the V content is increased as the amount of water is increased, see Table 2. These results show a different pattern compared with the previous results such as XRD and nitrogen physisorption. That is, the incorporated amount of V is increased with increasing water addition. This suggests that excess water in the synthesis solution may be helpful to obtain

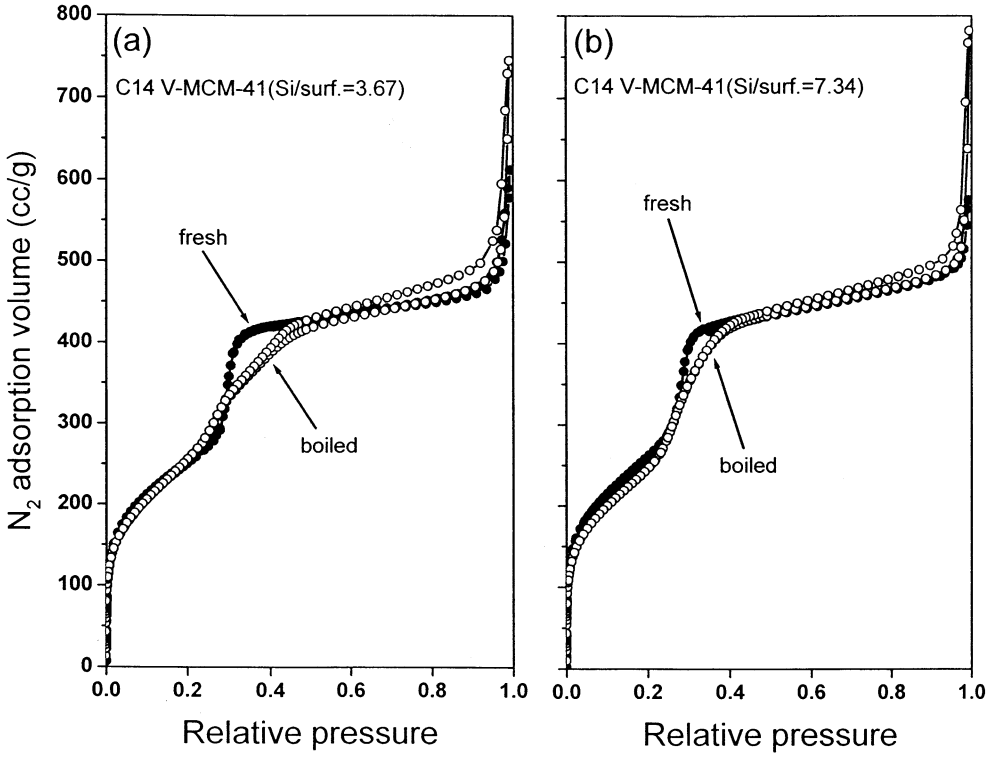

Figure 7. Comparison of nitrogen adsorption isotherms between fresh and boiled samples: (a) C14−MCM-41, Si/surf. = 3.67; (b) C14−MCM-41, Si/surf. = 7.34.

TABLE 1: Physical Properties of Prepared MCM-41 Samples

samples[a]	S_{BET} (m^2/g)	pore diameter (Å)	*d*-spacing (Å)	pore wall thickness (Å)
C10 V−MCM-41 (55.7)[a,b]	1039	18.2	30.3	16.8
C12 V−MCM-41 (27.0)[a,b]	1238	20.7	31.3	15.5
C12 V−MCM-41 (41.4)[a,b]	1278	20.7	31.2	15.3
C12 V−MCM-41 (55.7)[a,b]	1227	20.6	31.3	15.5
C12 V−MCM-41 (74.7)[a,b]	1238	20.8	31.3	15.3
C14 V−MCM-41 (55.7)[a,b]	1247	21.9	32.8	16.0
C16 V−MCM-41 (55.7)[a,b]	1106	25.9	37.4	17.2
C14 V−MCM-41 (74.7)[b,c]	932	25.4	35.4	15.6
C14 V−MCM-41 (74.7)[c,d]	921	24.8	35.4	16.1
C16 Si−MCM-41 (74.7)[b,c]	1074	26.0	38.3	18.2
C16 V−MCM-41 (74.7)[b,c]	938	27.2	40.0	18.9
C14 V−MCM-41 (74.7)[c,e]	536	25.4		
C14 V−MCM-41 (74.7)[c,f]	314	24.8		
C14 V−MCM-41 (74.7)[b,c,g]	926	24.0		
C14 V−MCM-41 (74.7)[c,d,g]	894	23.6		
C14 V−MCM-41 (74.7)[c,e,g]	564	33.4		
C14 V−MCM-41 (74.7)[c,d,h]	801	24.3		
C14 V−MCM-41 (74.7)[c,d,i]	812	24.9		
C14 V−MCM-41 (74.7)[c,d,j]	827	24.4		
C14 V−MCM-41 (74.7)[c,d,k]	788	24.4		
C14 V−MCM-41 (74.7)[c,d,l]	725	24.6		
C14 V−MCM-41 (74.7)[b,c,i]	850	25.5		
C14 V−MCM-41 (74.7)[b,c,j]	746	25.4		

[a] Values in parentheses represent water/Si mole ratio. [b] No pH adjustment, HiSil233. [c] Si/surf. mole ratio = 3.67. [d] pH adjustment, HiSil915. [e] Si/surf. mole ratio = 7.34. [f] Si/surf. mole ratio = 14.68. [g] Si/surf. mole ratio = 29.36. [h] Boiled in water for 24 h. [i] Pressed with 4391 lbs. [j] Pressed with 11437 lbs. [k] Pressed with 17000 lbs. [l] Pressed with 20000 lbs. [m] Pressed with 24000 lbs.

homogeneous mixing of reactants, and therefore, the incorporation of V may be facilitated when the reactant is in higher dilution in the aqueous synthesis solution. When the amount of V incorporation was measured as a function of the surfactant chain length, the longer the chain length, the higher the V content. These results seem to be more or less related with the bonding angle of V and Si. That is, if the chain length of surfactant is long enough it can form a large pore channel, and incorporated V can be arranged along the pore channel more easily than in the small pore channel templated by the short chain length surfactant. Therefore, it can be concluded that if high-V-content MCM-41 is desired, excess water may be added and long chain surfactant be used to promote V incorporation.

51V NMR Results. In the previous results, we saw that excess water did not affect the physical properties of V−MCM-41 samples but the incorporated amount of V was increased with increased addition of water in the synthesis solution. However, the analysis used does not tell us if the incorporated V is substituted into the silica framework to form a tetrahedral coordination with surrounding oxygen. Several ^{51}V NMR experiments were carried out to determine the V substitution state in the silica framework and the results are shown in Figure 9. All samples show a similar resonance pattern and the main signals are around −500 to −530 ppm which are assigned to tetrahedral coordinated V.[30] Octahedral coordination of V ions is not detected in these samples (chemical shift around −300 ppm). Thus, most of the incorporated V is substituted into the silica framework and assumes tetrahedral coordination with surrounding oxygen anions. However, all the main resonance peaks exhibit quite broad patterns compared to previously reported V-impregnated or -incorporated catalysts.[30,35−37] Initially, we attributed this to interference between signals. We carried out magic angle spinning (MAS) ^{51}V NMR for one sample (C16 V−MCM-41), but we could not find any differences between the static and MAS method. We chose another reference sample for static ^{51}V NMR, which has tetrahedral coordination (Na_3VO_4).[38] It shows a sharp and narrow resonance peak at around −570 ppm with the static method. This result indicates that all samples prepared in this study have some distorted or, perhaps disordered, tetrahedral coordination of V, so they show broad resonance peaks compared to the nondis-

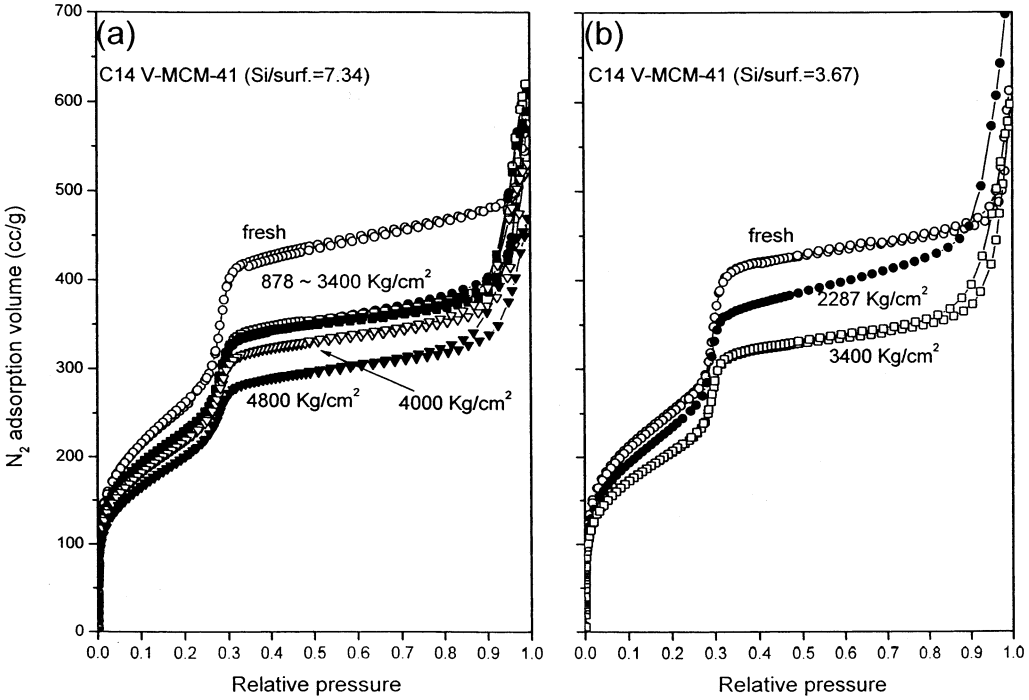

Figure 8. Nitrogen adsorption isotherms of fresh and pressed samples.

TABLE 2: Results of Chemical Analysis (ICP) for V−MCM-41 Samples Prepared in This Study

samples	analysis	results (wt %)	Si/V mole ratio
C10 V−MCM-41 (H_2O/Si mole ratio = 55.7)	vanadium	0.41	207.5
C12 V−MCM-41 (H_2O/Si mole ratio = 27.0)	vanadium	0.82	102.7
C12 V−MCM-41 (H_2O/Si mole ratio = 41.4)	vanadium	0.88	95.8
C12 V−MCM-41 (H_2O/Si mole ratio = 55.7)	vanadium	0.92	91.7
C12 V−MCM-41 (H_2O/Si mole ratio = 74.7)	vanadium	1.03	81.7
C14 V−MCM-41 (H_2O/Si mole ratio = 55.7)	vanadium	1.10	76.3
C16 V−MCM-41 (H_2O/Si mole ratio = 55.7)	vanadium	1.77	47.2

torted sample. When water addition is increased to a H_2O/Si mole ratio of 74.7, the main signal is shifted a little lower because of the additional distortion of tetrahedral structure attributed to the higher content of V. Alternatively, this may reflect a distribution of tetrahedral environments. All spectra show additional signals at around −820 to −950 ppm and they shift to a higher value with increasing surfactant chain length. These are also likely to be distorted tetrahedral structures[30] and they seem to depend on the pore size, and thus perhaps the associated V−O−Si bonding angle.

Acidic Properties of V−MCM-41. The acidic properties of synthesized V−MCM-41 samples were investigated by pyridine TPD and in-situ FTIR. We have used pyridine as a probe molecule in order to compare the results in the in-situ FTIR, directly, to determine the kind of acid sites. As shown in Figure 10, all V−MCM-41 samples show two kinds of pyridine desorption peaks at around 250 °C and 380 °C. This implies that V−MCM-41 has acid sites of different acid strength on the surface. The first peak at around 250 °C is of similar size for all samples and its concentration is about $(2.8-2.9) \times 10^{-5}$ mol/g when it was quantified. The second peak increases with increasing amount of V incorporated into the silica framework. Therefore, it may be assumed that the second peak can be attributed to the incorporated V only. Initially, the first peak was attributed to pyridine adsorbed on silanol groups. However, the size of the 250 °C peak of pure siliceous MCM-41 is only half that of the V−MCM-41 samples. This suggests that the 250 °C peak of V−MCM-41 may consist of the pyridinium ion adsorbed on a acid site and hydrogen-bonded pyridine with free silanol groups.

To confirm the kinds of acid sites of V−MCM-41, the in-situ FTIR of pyridine adsorption was carried out for the C16 V−MCM-41 sample. Figure 11a shows the absorbance patterns in the hydroxyl group region at each temperature. There are huge peaks around 3300∼3600 cm^{-1} at room temperature, which are assigned to the hydrogen-bonded hydroxyl group on the silica surface.[39,40] As the evacuation temperature is increased, the hydrogen-bonded OH group disappears and there remain only free silanol groups at 400 °C. In this study, the sample pretreatment temperature was 500 °C. Therefore we may ignore the effects of hydrogen-bonded hydroxyl groups when pyridine is adsorbed on the surface of V−MCM-41. Any sulfur or sulfur oxide compounds were not seen in the IR spectra. Therefore, we could confirm that there is no sulfuric compound, which is a possible impurity from the vanadium precursor, on the V−MCM-41 sample prepared in this study. Pyridine was adsorbed at 150 °C on C16 V−MCM-41 and the absorbance patterns were investigated with increasing evacuation temperature as shown in Figure 11b. At 150 °C, which is the pyridine adsorption temperature, there are 4 main peaks assigned to physisorbed pyridine at around 1600 cm^{-1}, pyridinium ion adsorbed on the Brönsted acid sites at around 1540 cm^{-1}, pyridinium ion adsorbed on the Brönsted and Lewis acid sites at around 1480 cm^{-1}, and pyridine associated with Lewis acid sites and pyridine on the free silanol groups at around 1448 cm^{-1}.[41−45] When the sample was evacuated at 200 °C, which is the temperature just before the first peak of pyridine TPD, there are still four peaks on the surface of V−MCM-41 although all peak intensities are severely decreased. However, when it was evacuated at 300 °C, which is the temperature just after the first peak of pyridine TPD, the peak of the Lewis acid sites disappeared completely, but the Brönsted acid sites still remain on the V−MCM-41 surface. This demonstrates that the first peak of pyridine TPD mainly consists of the Lewis acid sites and the acid sites of the second peak are mostly Brönsted acid

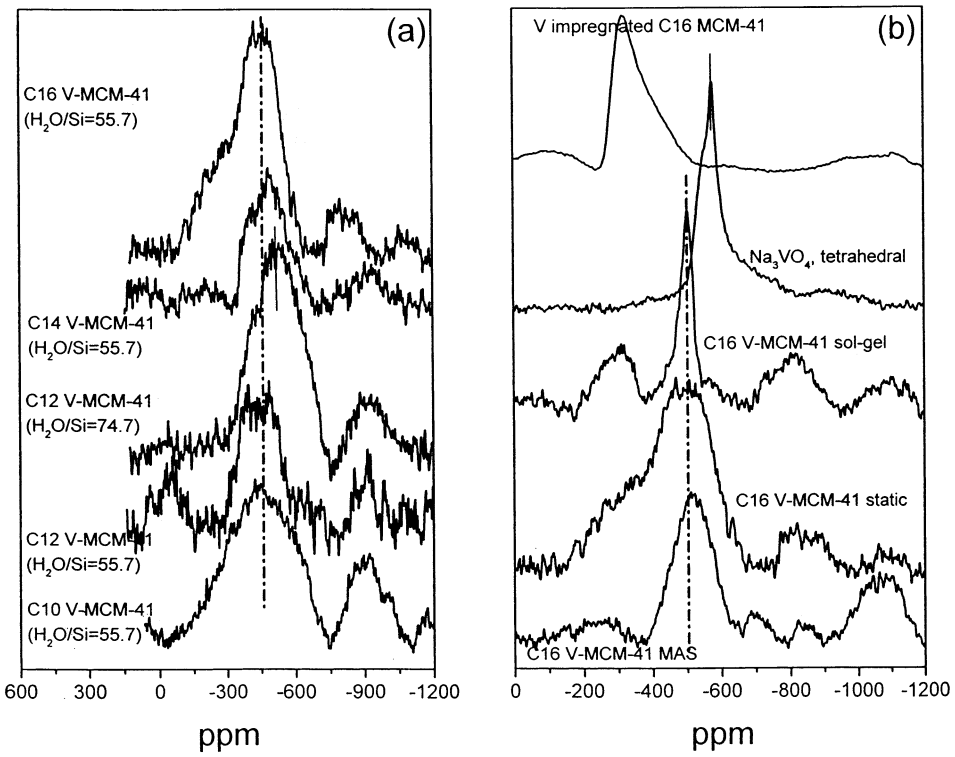

Figure 9. ^{51}V NMR spectra patterns of V−MCM-41 samples: (a) static, (b) static and magic angle spinning.

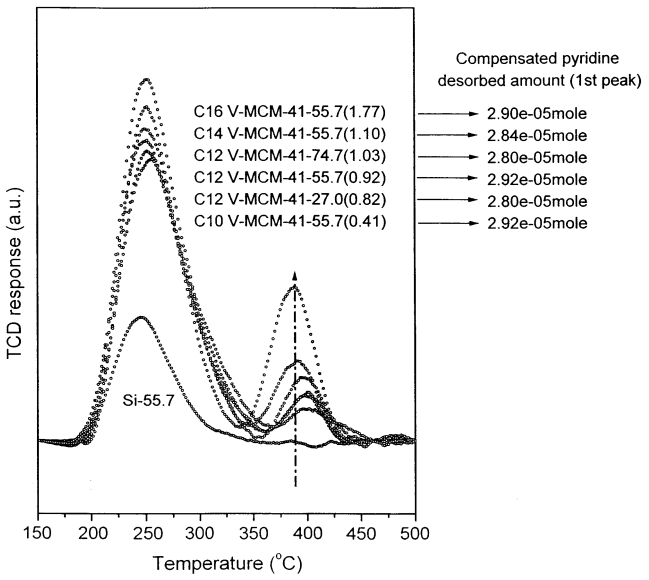

Figure 10. Pyridine temperature-programmed desorption (TDP) patterns of V−MCM-41 samples: surfactant chain length V−MCM-41−H_2O/Si mole ratio (vanadium wt %).

sites formed by V, which are combined with the free silanol group. We could not find any strong Lewis acid sites at around 1455 cm^{-1}, a frequency attributed to the octahedrally coordinated vanadium oxide on the surface.[44,45] Therefore, we hypothesize that the Lewis acid sites are weak acid sites, which are tetrahedrally coordinated V, consistent with the result from ^{51}V NMR. Finally, we suggest that the weak Lewis acid sites are formed by isolated tetrahedral coordination of V and their amount is independent of the V content in V−MCM-41. It is suggested that there may be a constant number of sites which are potentially isolated Lewis acid sites in the silica framework and these are converted and saturated by the amount of V added. MCM-41 has an amorphous pore wall structure, similar to precipitated silica, and it exhibits characteristics different from

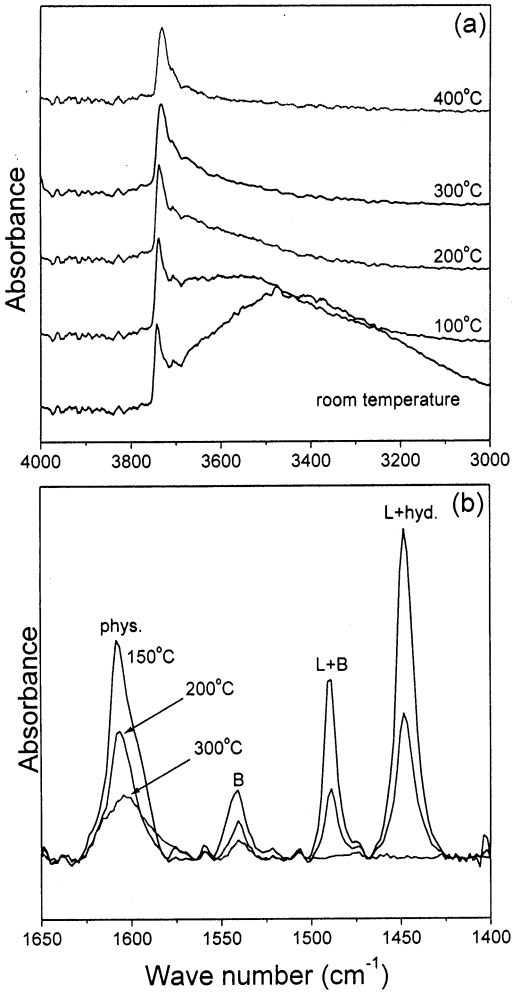

Figure 11. In-situ FTIR spectra patterns of C16 V−MCM-41: (a) OH group region; (b) acid site region after pyridine adsorption at 150 °C.

crystalline zeolite. The constant density of Lewis acid sites is probably due to the structural defects of the amorphous silica framework. It may be assumed that these acid sites would be correlated with the catalytic activities of this sample. We are investigating this effect by changing the amount of silica source. The Brönsted acid sites may possibly be formed by combining with the dissociated water molecule of a hydrogen-bonded silanol group when the sample is pretreated.

Conclusions

Highly ordered V-substituted MCM-41 was prepared and its physicochemical properties were investigated. From the results of XRD and N_2 physisorption, it was found that an anti-foaming agent is a very useful additive to increase sample reproducibility, and that excess water addition to the synthesis solution does not affect the physical properties of V−MCM-41 samples in the presence of the anti-foaming agent. The hydrothermal and mechanical stability was increased when the pH was adjusted to 11 (Si/surfactant mole ratio = 7.34). All samples have similar pore wall thickness of 10−11 Å regardless of the surfactant chain length. By chemical analysis (ICP) of the samples, it was found that the V content was increased with increased water addition, probably due to the enhancement of mixing (lower viscosity). Essentially, all V incorporated into the siliceous MCM-41 was substituted into the silica framework and resulted in a small amount of disordered tetrahedral coordination with surrounding oxygen. From the results of pyridine TPD and in-situ FTIR, it was found that the V−MCM-41 samples prepared in this study have both Lewis and Brönsted acid sites on the surface. The Lewis acid sites of these samples are weak and appear to be coordinated tetrahedrally with oxygen and their amount was constant regardless of the incorporated V amount.

Acknowledgment. We are grateful to the Office of Basic Energy Science, DOE, for financial support. A partial postdoctoral stipend for one of us (S. Lim) was provided by the Korea Research Foundation.

References and Notes

(1) Kresge, C. T.; Leonowicz, M. E.; Roth, W. J.; Vartuli, J. C.; Beck, J. S. *Nature* **1992**, *359*, 710.
(2) Beck, J. S.; Vartuli, J. C.; Roth, W. J.; Leonowicz, M. E.; Kresge, C. T.; Schmit, K. D.; Chu, C. T.-W.; Olson, D. H.; Sheppard, E. W.; McCullen, S. B.; Higgins, J. B.; Schlenker, J. L. *J. Am. Chem. Soc.* **1992**, *114*, 10834.
(3) Schmidt, R.; Akporiaye, D.; Stöcker, M.; Ellestad, O. H. *J. Chem. Soc., Chem. Commun*. **1994**, 1493.
(4) Yuan, Z. Y.; Liu, S. Q.; Chen, T. H.; Wang, J. Z.; Li, H. X. *J. Chem. Soc., Chem. Commun*. **1995**, 973.
(5) Das, T. K.; Chaudhari, K.; Chandwadkar, A. J.; Sivasanker, S. *J. Chem. Soc., Chem. Commun*. **1995**, 2495.
(6) Cheng, C. F.; Klinowski, J. *J. Chem. Soc., Faraday Trans*. **1996**, *92*, 289.
(7) Cheng, C. F.; He, H.; Zhou, W.; Klinowski, J.; Gonçalves, J. A. S.; Gladden, L. F. *J. Phys. Chem*. **1996**, *100*, 390.
(8) On, D. T.; Joshi, P. N.; Kaliaguine, S. *J. Phys. Chem*. **1996**, *100*, 6743.
(9) Alba, M. D.; Luan, Z.; Klinowski, J. *J. Phys. Chem*. **1996**, *100*, 2178.
(10) Ulagappan, N.; Rao, C. N. R. *Chem. Commun*. **1996**, 1047.
(11) Aguado, J.; Serrano, D. P.; Romero, M. D.; Escola, J. M. *Chem. Commun*. **1996**, 725.
(12) Hartmann, M.; Pöppl, A.; Kevan, L. *Stud. Surf. Sci. Catal*. **1996**, *101*, 801.
(13) Armengol, E.; Cano, M. L.; Corma, A.; Garcia, H.; Navarro, M. T. *J. Chem. Soc., Chem. Commun*. **1995**, 519.
(14) Junges, U.; Jacobs, W.; Martin, I. V.; Krutzsch, B.; Schüth, F. *J. Chem. Soc., Chem. Commun*. **1995**, 2283.
(15) Corma, A.; Navarro, M. T.; Pariente, J. P. *J. Chem. Soc., Chem. Commun*. **1994**, 147.
(16) Emerson, S. C.; Klocke, D. J. U.S. Patent 5,538,711, 1996.
(17) Chen, X.; Huang, L.; Li, Q. *J. Phys. Chem. B* **1997**, *101*, 8460.
(18) Huo, Q.; Margolese, D. I.; Stucky, G. D. *Chem. Mater*. **1996**, *8*, 1147.
(19) Kim, J. M.; Kwak, J. H.; Jun, S.; Ryoo, R. *J. Phys. Chem*. **1995**, *99*, 16742.
(20) Gusev, V. Y.; Feng, X.; Bu, Z.; Haller, G. L.; O'Brien, J. A. *J. Phys. Chem*. **1996**, *100*, 1985.
(21) Tatsumi, T.; Koyano, K. A.; Tanaka, Y.; Nakata, S. *J. Porous Mater*. **1999**, *6*, 13.
(22) Hartmann, M.; Bischof, C. *J. Phys. Chem. B* **1999**, *103*, 6230.
(23) Reddy, K. M.; Moudrakovski, I.; Sayari, A. *J. Chem. Soc., Chem. Commun*. **1994**, 1059.
(24) Chao, K. J.; Wu, C. N.; Chang, H.; Lee, L. J.; Hu, S. F. *J. Phys. Chem. B* **1997**, *101*, 6341.
(25) Ravikovitch, P. I.; Wei, D.; Chueh, W. T.; Haller, G. L.; Neimark, A. V. *J. Phys. Chem. B* **1997**, *101*, 3671.
(26) Park, D. H.; Cheng, C. F.; Klinowski, J. *B. Kor. Chem. Soc*. **1997**, *18*, 70.
(27) Park, D. H.; Cheng, C. F.; He, H.; Klinowski, J. *J. Mater. Chem*. **1997**, *7*, 159.
(28) Neumann, R.; Khenkin, A. M. *Chem. Commun*. **1996**, 2643.
(29) Sayari, A.; Karra, V. R.; Reddy, J. S.; Moudrakovski, I. L. *Adv. Porous Mater. Res. Soc. Symp. Proc*. **1995**, *371*, 81.
(30) Eckert, H.; Wachs, I. E. *J. Phys. Chem*. **1989**, *93*, 6796.
(31) Gonzalez, R. D.; Lopez, T.; Gomez, R. *Catal. Today* **1997**, *35*, 293.
(32) Morey, M.; Davidson, A.; Eckert, H.; Stucky, G. *Chem. Mater*. **1996**, *8*, 486.
(33) Grubert, G.; Rathousky, J.; Schulz-Ekloff, G.; Wark, M.; Zukal, A. *Microporous Mesoporous Mater*. **1998**, *22*, 225.
(34) Lim, S.; Haller, G. L. *Appl. Catal.* A **1999**, *188*, 277.
(35) Reddy, J. S.; Liu, P.; Sayari, A. *Appl. Catal. A* **1996**, *148*, 7.
(36) Sen, T.; Ramaswamy, V.; Ganapathy, S.; Rajamohanan, P. R.; Sivasanker, S. *J. Phys. Chem.* **1996**, *100*, 3809.
(37) Rigutto, M. S.; Bekkum, H. V. *J. Mol. Catal*. **1993**, *81*, 77.
(38) Rehr, J. J.; Booth, C. H.; Bridges, F.; Zabinski, S. I. *Phys. Rev. B* **1994**, *49*, 12347.
(39) Zhao, X. S.; Lu, G. Q.; Whittaker, A. K.; Millar, G. J.; Zhu, H. Y. *J. Phys. Chem. B* **1997**, *101*, 6525.
(40) On, D. T.; Joshi, P. N.; Lemay, G.; Kaliaguine, S. *Stud. Surf. Sci. Catal*. **1997**, *97*, 543.
(41) Mokaya, R.; Jones, W. *Chem. Commun*. **1996**, 983.
(42) Mokaya, R.; Jones, W.; Luan, Z.; Alba, M. D.; Klinowski, J. *Catal. Lett*. **1996**, *37*, 113.
(43) Climent, M. J.; Corma, A.; Iborra, S.; Navarro, M. C.; Primo, J. *J. Catal*. **1996**, *161*, 783.
(44) Renzo, F. D.; Chiche, B.; Fajula, F.; Viale, S.; Garrone, E. *Stud. Surf. Sci. Catal*. **1996**, *101*, 851.
(45) Jentys, A.; Pham, N. H.; Vinek, H. *J. Chem. Soc., Faraday Trans*. **1996**, *92*, 3287.